Journal of Nano- and Electronic Physics
Vol. **11** No 2, 02033(8pp) (2019)
Журнал нано- та електронної фізики
Том **11** № 2, 02033(8сс) (2019)

Modelling of Vibration Sensor Based on Bimorph Structure

M.D. Malinkovich[1,*], I.V. Kubasov[1], A.M. Kislyuk[1], A.V. Turutin[1], A.S. Bykov[1], D.A. Kiselev[1], A.A. Temirov[1], R.N. Zhukov[1], N.A. Sobolev[1,2], B.M.S. Teixeira[2], Yu.N. Parkhomenko[1]

[1] *Department of the Materials Science of Semiconductors and Dielectrics, National University of Science and Technology MISiS, 119049 Moscow, Russia*
[2] *Department of Physics and I3N, University of Aveiro, 3810-193 Aveiro, Portugal*

(Received 18 January 2019; revised manuscript received 11 March 2019; published online15 April 2019)

In the current study, we have developed a mathematical model describing the frequency response of a sensor or energy harvester based on a cantilever made of a ferroelectric bidomain single-crystal plate with metal electrodes deposited on opposite faces. The structure is subjected to vibrational excitations. The model allows to predict the dependence of the voltage between the electrodes vs. the vibration frequency and amplitude as well as resonance frequency of the sensor fabricated in form of a rectangular plate, normally with a seismic mass on its free end. The device is placed on a vibration table, whose vibration parameters are set. The relevant differential equation was composed, and an analytic solution describing the required dependencies was obtained. To validate the proposed model, we created a single-crystal bimorph by annealing a lithium niobate ($LiNbO_3$) wafer in air to promote Li out-diffusion and formation of a bidomain ferroelectric structure, i.e. two oppositely polarized domains within the plate (the so called "head-to-head" structure). Such a crystal demonstrates a bimorph-like behavior but does not comprise any interface except for an interdomain wall. Thus, our bimorph is not a commonly used structure, typically consisting of two bonded piezoelectric plates (generally made of PZT piezoceramics), but a homogeneous continuous medium. Being made of a lithium niobate (or lithium tantalate) ferroelectric single crystal, the cantilever sensor or energy harvester demonstrates a strong dependence of the voltage between the electrodes on the bending deformations, with almost totally absent hysteresis and ageing in a wide temperature range. The comparison made between the results of the modeling and the experiment shows that the proposed model is in good agreement with the experiment. We have demonstrated that the vibration sensors based on bidomain single-crystal plates possess an exceptionally high sensitivity. The proposed model can be used to estimate and predict the parameters of vibration sensors, accelerometers and waste energy harvesters based on bidomain ferroelectric crystals.

Keywords: Bimorph, Bidomain crystal, Vibration sensor, Energy harvesting, Modelling.

DOI: 10.21272/jnep.11(2).02033 PACS numbers: 77.65.– j, 02.30.Hq

1. INTRODUCTION

In the past 10-15 years there is an increased interest to converting the mechanical energy of vibrations and random pulses into electrical energy. A large number of such converters [1] have been proposed, most of them based on the use of cantilevered piezoelectric beams [2, 3]. The cantilevers proposed by all the authors have nearly the same structure [4, 5]: they consist of a substrate, mostly metallic, to one surface of which, along the full length of it or partially, a thin piezoceramic plate with a top electrode is attached (glued). As the cantilever vibrates, electrical voltage is generated between the top electrode and the substrate. Occasionally, a bimorph scheme is used, where piezoelectric plates are attached to both sides of the metallic substrate (so-called parallel bimorph), whereby the voltage is measured between electrodes applied to piezoelectric plates, and the substrate [3].

Multiple mathematical models, describing vibrating cantilevers under external excitations, based on the Euler-Bernoulli beam equation, have been proposed. The most complete description of such an approach was given in the monograph [6]. More recent works essentially reproduce and develop conceptual issues proposed by these authors using multiple constructions and configurations of energy harvesters.

Although many different types of cantilevers having different shapes and arrangements of piezoelectric and passive layers were offered, only few materials were tested. Indeed, in almost all studies the same piezoelectric material PZT (lead zirconate-titanate) was used. Even though single-crystal piezoelectric materials (such as quartz, langasite, yttrium oxyborate, lithium niobate or lithium tantalate) exhibit a higher thermal stability and less internal damping than PZT [7], their main disadvantage – low values of piezoelectric coefficients – is the reason why PZT is still used in most cases.

Previously [8] we have established a methodology for creating a bidomain structure in plates of lithium niobate and lithium tantalate single-crystal ferroelectrics and studied their electromechanical characteristics [9]. Such "bidomain" crystals demonstrate a bimorph-like behavior but do not comprise any interface except for an interdomain wall. Bending deformation of this single-crystal bimorph causes the expansion of one domain and contraction of its counterpart. The voltages induced in the domains by the direct piezoelectric effect are added up; they are proportional to the bending magnitude at a fixed frequency.

It has been experimentally demonstrated that the bending strain dependence on the voltage applied to electrodes of a bidomain plate is marked by high linear-

* malinkovich@yandex.ru

ity, and the coupling factor is comparable to the values specific for piezoceramic materials. In particular, this enabled a successful application of lithium niobate plates with a bidomain structure in an X-ray focusing system. Additionally, owing to a weak piezoelectric coefficient dependence on the temperature, along with high Curie temperatures, bimorphs based on such materials in some cases (e.g. as vibration sensors or energy harvesters) can be more effective and have a broader application than those based on piezoceramics. In our recent works we have reported the results of applying piezoelectric cantilevers made of lithium niobate single-crystal bidomain plates as highly sensitive vibration sensors. We have demonstrated that in several aspects including sensitivity they considerably exceed the sensors on the basis of piezoceramics. Moreover, due to symmetry of piezoelectric effect the same crystals can be used not only in vibrational sensors but also in energy harvesters, including beta-voltaic generators [10], and in magnetic field sensors based on composite multiferroics [11].

In the current work we propose a model of a sensor for monitoring vibrations excited by an external source on the basis of lithium niobate and/or lithium tantalate bidomain single crystals and provide a comparison of estimated frequency-voltage characteristics and Q-factor with experimental data. The main difference from earlier models consists in the consideration of the piezoelectric material not as a part of some composite structure but as an entire cantilevered energy harvester or vibration sensor. This model also incorporates a possible presence of the interdomain region between the domains [8] and is applicable to any other ferroelectric materials with a bidomain structure.

2. PHENOMENOLOGICAL DESCRIPTION OF BIDOMAIN PIEZOELECTRIC CANTILEVER

2.1 Problem Statement and Basic Equations

We consider the rectangular bidomain beam shown in Fig. 1, which is simply a cantilever fixed at one of its ends. There is a seismic mass fastened onto the tip of the bimorph. The dimensions of the cantilever are $L \times W \times H$ and those of the seismic mass m^* are $l \times w \times h$.

Oscillations of the cantilever occur due to the periodic displacements of the base. The balance of the torques is represented by the equation:

$$\mathbf{M}_b + \mathbf{M}_s + \mathbf{M}_f = \mathbf{I}\ddot{\varphi}, \qquad (1)$$

where $\mathbf{M}_b$ is the bending moment, $\mathbf{M}_s$ is the moment of the elastic force, $\mathbf{M}_f$ is the moment of friction, $\mathbf{I}$ is the moment of inertia of the cantilever, $\ddot{\varphi}$ is the angular acceleration. The bending moment is the sum of the moment of the cantilever weight which is applied to its center (in the case of a uniform beam), and the moment associated with a seismic mass or an external force (e.g. electrostatic) which is applied to the point located at a distance of $l/2$ from the free end of the cantilever. Therefore, the bending moment can be expressed as:

$$|\mathbf{M}_b| = \frac{mgL}{2} + FL\left(1 - \frac{\xi}{2}\right), \qquad (2)$$

where m is the mass of the cantilever, g is the acceleration of the crystal which is a sum of the gravity acceleration g_0 and acceleration of the base, F is the seismic mass weight or another external force, and $\zeta = l/L$.

The moment of the elastic force can be represented as:

$$|\mathbf{M}_s| = Lkz, \qquad (3)$$

where k is the stiffness of the beam, and z represents the deflection of the tip of the cantilever.

Moment of friction can be expressed as:

$$|\mathbf{M}_f| = L\gamma\dot{z}, \qquad (4)$$

where γ is the constant describing speed-proportional damping in the system.

Moment of inertia of the cantilever fixed at one end relatively to the line of attachment is calculated as follows:

$$|\mathbf{I}| = \int_0^{L-l} \rho W H x^2 dx + \int_{L-l}^{L} \left(\rho W H + \rho^* wh\right) x^2 dx = \frac{\rho W H L^3}{3} + \frac{\rho^* wh L^3}{3} + \frac{\rho^* wh}{3}\left(L^3 - 3L^2 l + 3Ll^2 - l^3\right) = \frac{L^2}{3}\left[m + m^*\left(\xi^2 - 3\xi + 3\right)\right] = \frac{m_{eff} L^2}{3}, \qquad (5)$$

where we considered a rectangular seismic mass having a height of h, width of $w = W$ and density of ρ^* and introduced the effective mass $m_{eff} = \left[m + m^*\left(\xi^2 - 3\xi + 3\right)\right]$.

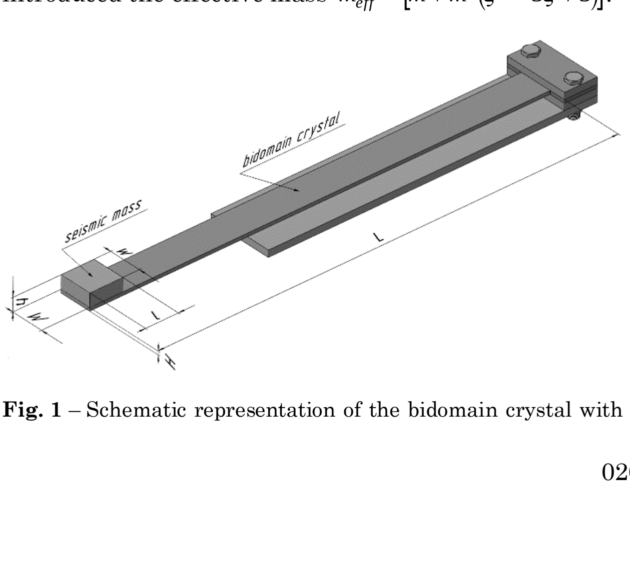

Fig. 1 – Schematic representation of the bidomain crystal with a seismic mass at the tip fastened in a clamp

When the oscillation amplitude of the cantilever is small ($z << L$), then the angle $\varphi \approx z/L$, and the angular acceleration is $\ddot{\varphi} \approx \ddot{z}/L$. Thus, equation (1) takes the form (considering the signs):

$$\frac{mgL}{2} + FL\left(1 - \frac{\xi}{2}\right) - Lkz - L\gamma\dot{z} = \frac{m_{eff} L^2}{3}\frac{\ddot{z}}{L}$$

or even easier:

$$\frac{mg}{2} + F\left(1 - \frac{\xi}{2}\right) - kz - \gamma\dot{z} = \frac{m_{eff}}{3}\ddot{z}. \qquad (6)$$

In case of the external vibrational source producing harmonic excitations with a displacement of $d = d_0 \sin(\omega t)$ and considering the presence of the seismic mass m^* we obtain $F = m^* g = m^*\left(g_0 + \ddot{d}\right)$, and equation (6) takes the form:

$$\ddot{z} + 2\chi\omega_0 \ddot{z} + \omega_0^2 z = \beta - \delta \sin(\omega t). \qquad (7)$$

Here we used the next substitutions:

$$\left[\frac{m}{2} + m^*\left(1 - \frac{\xi}{2}\right)\right] = m_1,$$

$$\frac{m_1 d_0 \omega^2}{m} = \delta,$$

$$\frac{m_{eff}}{3} = \overline{m},$$

$$\frac{k}{\overline{m}} = \omega_0^2,$$

$$\frac{g_0 m_1}{\overline{m}} = \beta,$$

$$\frac{\gamma}{\overline{m}} = 2\chi\omega_0.$$

Solving equation (7) with regard to the substitutions, we find the dependence of deflection of the cantilever free end on the beam parameters and on the frequency and amplitude of the external vibrational excitation:

$$z(t) = d_0 \frac{\omega}{\omega_0} \cdot \frac{1}{\sqrt{1-\chi^2}} e^{-\chi\omega_0 t} \sin\left(\omega_0 t \sqrt{1-\chi^2}\right) - d_0 \frac{m_1}{\overline{m}} \cdot \frac{\omega^2}{\omega_0^2} \cdot \frac{1}{\sqrt{\left(1 - \frac{\omega^2}{\omega_0^2}\right)^2 + 4\chi^2 \frac{\omega^2}{\omega_0^2}}} \sin(\omega t - \theta) + g_0 \frac{m_1}{\overline{m}} \cdot \frac{1}{\omega_0^2}, \qquad (8)$$

where we denoted $\theta = \tan^{-1}\left[2\chi\omega_0\omega / \left(\omega_0^2 - \omega^2\right)\right]$.

The damping parameter χ can be experimentally determined from the quality factor Q of the system. Indeed, when the damping is relatively small ($4\chi\pi < 1$), the Q-factor can be approximately taken to be:

$$Q \approx \frac{1}{2\chi}. \qquad (9)$$

The fist bending resonance frequency of the vibrating cantilever with the seismic mass can be calculated using the equation:

$$\omega_0 = \sqrt{\frac{k}{\overline{m}}} = \sqrt{\frac{3E_Y I_x \left[4\frac{m}{m+m^*} + 3\left(1 - \frac{l}{2L}\right)\frac{m^*}{m+m^*}\right]}{L^3\left\{m + m^*\left[\left(\frac{l}{L}\right)^2 - 3\frac{l}{L} + 3\right]\right\}}}, \qquad (10)$$

where the area moment of inertia is $I_x = (WH^3)/12$, and E_Y is Young's modulus which is determined by the material of the cantilever and its crystal cut.

2.2 Voltage Across the Bidomain Plate

Oscillations of the base with the fastened cantilever under the influence of an external vibration source will cause a periodic deformation of the bidomain crystal and generation of voltage at the electrodes deposited onto the opposite faces of the beam. When the oscillating cantilever is bent, e.g., downwards, as it is shown in Fig. 2a, then the electric fields E_1 and E_2 are induced in each of the domains. If the bidomain crystal plate possess an interdomain region with multidomain ferroelectric structure or uneven domain boundary, then the strain-induced electric fields in the interdomain region are zero on an average. The voltage magnitude depends on the "quality" of the bidomain structure, i.e. on the symmetry of the domains relatively to the middle section of the plate and their volumes. In order to calculate the voltage induced by bending the beam, we introduce the y axis that is perpendicular to the neutral plane of the plate in each cross section of the cantilever (Fig. 2b).

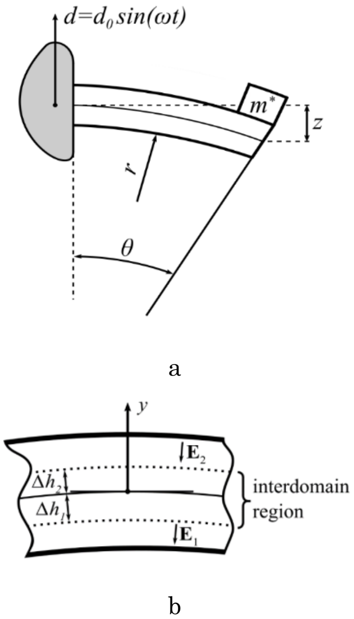

Fig. 2 – Bending of the cantilever under the vibrational excitation (a) and electric fields induced by the deformation of the bidomain crystal having an interdomain region (b)

The voltage U at the electrodes of the bidomain plate can be calculated as follows:

$$U = -\int_{-\frac{H}{2}}^{\frac{H}{2}} E(y)dy = -\left[\int_{-\frac{H}{2}}^{\Delta h_1} E_1(y)dy + \int_{\Delta h_2}^{\frac{H}{2}} E_2(y)dy\right], \qquad (11)$$

where $E = E_1 + E_2$ is a resulting electric field, Δh_1 and Δh_2 are the distances from the neutral plane of the plate to the lower and upper domains, respectively (the sum $\Delta h_1 + \Delta h_2$ is the width of the interdomain region).

Absolute values of the electric field in the domains depend on the distance y from the neutral plane of the bidomain plate, as:

$$E(y) = \frac{P(y)}{\varepsilon\varepsilon_0} = \frac{d_{ij} T_{ij}(y)}{\varepsilon\varepsilon_0} = \frac{d_{ij} E_Y S(y)}{\varepsilon\varepsilon_0}, \qquad (12)$$

where $P(y)$ is the magnitude of the electric polarization vector, ε and d_{ij} are the dielectric permittivity and matrix of piezoelectric coefficients of the cantilever material, respectively, $\varepsilon_0 = 8.854$ pF/m is the permittivity of the free space, $T_{ij}(y)$ and $S(y)$ are the dependencies of the mechanical stress and strain in the direction of the plate length on the y coordinate, respectively.

For small deformations the strain $S(y)$ can be represented as:

$$S(y) = \frac{\Delta L(y)}{L} = \frac{(r+y)\theta - r\theta}{L} = \frac{y\theta}{L}\,, \tag{13}$$

where $\Delta L(y)$ is the elongation of the plate at the coordinate y, r is the radius of curvature of the bended plate, θ is the angle between the radii drawn to the fixed and free end of the plate. The deflection z at the tip of the cantilever can be represented through the radius of curvature r of the plate and the angle θ (see Fig. 2):

$$S(y) = \frac{2y}{L^2} z\,, \tag{14'}$$

$$S(y) = -\frac{2y}{L^2} z\,, \tag{14''}$$

respectively.

Substituting (14') and (14'') into (12), and then into (11), one can determine the voltage on the electrodes of the bidomain plate depending on the deviation of the free end of the plate:

$$U = \frac{d_{ij}E_Y}{\varepsilon\varepsilon_0 L^2}\left[\frac{H^2}{2} - \left(\Delta h_1^2 + \Delta h_2^2\right)\right] z\,. \tag{15}$$

Another way to consider the imperfection of the bidomain crystal is utilizing the so-called "k-factor" which describes the effective value of the piezoelectric coefficient d_{ij} that can be calculated from the deflection of the tip when a constant voltage is applied. The detailed description of this approach can be found in [10].

Obviously, if a bidomain crystal does not possess an interdomain region, or this region is very narrow, the terms Δh_1 and Δh_2 are equal to zero, and equation (15) simply transforms into:

$$U = \frac{d_{ij}E_Y}{2\varepsilon\varepsilon_0}\left(\frac{H}{L}\right)^2 z\,. \tag{15'}$$

Combining equations (8) and (15) and considering that z is a function of time for an oscillating cantilever, one can obtain the final equation for the calculation of the voltage:

$$U(\omega,t) = \frac{d_{ij}E_Y}{\varepsilon\varepsilon_0 L^2}\left[\frac{H^2}{2} - \left(\Delta h_1^2 + \Delta h_2^2\right)\right] \times \left[g_0 \frac{m_1}{\overline{m}} \cdot \frac{1}{\omega_0^2} + d_0 \frac{\omega}{\omega_0} \cdot \frac{1}{\sqrt{1-\chi^2}} e^{-\chi\omega_0 t} \sin\left(\omega_0 t\sqrt{1-\chi^2}\right) - d_0 \frac{m_1}{\overline{m}} \cdot \frac{\omega^2}{\omega_0^2} \cdot \frac{1}{\sqrt{\left(1-\frac{\omega^2}{\omega_0^2}\right)^2 + 4\chi^2\frac{\omega^2}{\omega_0^2}}} \sin(\omega t - \theta) \right]. \tag{16}$$

As it follows from equation (16), the open-circuit voltage generated by the vibrating bidomain cantilever contains:

(i) constant part associated with a static deflection of the beam under its own weight and weight of the seismic mass;

(ii) rapidly attenuating part associated with the settling of the oscillations during the starting periods of the vibrational excitation;

(iii) harmonic part with the frequency of the vibrational excitation ω and the phase shift θ.

The origin of the part (i) is the fact that we did not consider the finite resistance of the bidomain crystal, therefore in the case of a real crystal the voltage induced by a static bending is compensated by internal and external free charges, and the part (i) is equal to zero. The part (ii) in equation (16) decreases rapidly even if the Q-factor is relatively large, therefore it can be neglected in measurements of steady-state vibrations. It is also convenient to operate not with the angular frequency ω, but with the frequency $f = \omega/2\pi$. Considering the above-mentioned simplifications and equation (9), we can rewrite (16) in the next form:

$$U(f,t) = \frac{d_{ij}E_Y d_0}{\varepsilon\varepsilon_0 L^2} \cdot \frac{m_1}{\overline{m}} \cdot \left(\frac{f}{f_0}\right)^2 \cdot \left[\frac{H^2}{2} - \left(\Delta h_1^2 + \Delta h_2^2\right)\right] \cdot \frac{1}{\sqrt{\left\{1-\left(\frac{f}{f_0}\right)^2\right\}^2 + \frac{1}{Q^2}\left(\frac{f}{f_0}\right)^2}} \sin(2\pi f t - \theta). \tag{17}$$

The final formula for the frequency response of the bidomain cantilever can be obtained simply taking the magnitude of the sine function in the right part of equation (17):

$$U(f) = \frac{d_{ij} E_Y d_0}{\varepsilon\varepsilon_0 L^2} \cdot \frac{m_1}{\overline{m}} \frac{\left(\frac{f}{f_0}\right)^2 \cdot \left[\frac{H^2}{2} - \left(\Delta h_1^2 + \Delta h_2^2\right)\right]}{\sqrt{\left\{1 - \left(\frac{f}{f_0}\right)^2\right\}^2 + \frac{1}{Q^2}\left(\frac{f}{f_0}\right)^2}} \quad (18)$$

As it follows from equation (18), the problem of the vibration sensor modeling is reduced to the determination of the cantilever domain structure and the time dependence of its free end movement on the frequency and amplitude of the external excitation.

3. EXPERIMENTAL VALIDATION

In this section we provide an experimental validation of the proposed analytical relationships. The experimentally measured voltage response to vibrations of the base with the fastened single-crystal bimorph is compared with the data predicted by equation (18).

The bimorph for the study was produced of a $LiNbO_3$ single-crystal wafer (ELAN Company Ltd, Russia) having the y + 128° crystallographic orientation. Two oppositely polarized ferroelectric domains (so-called "head-to-head" bidomain structure) were formed in the plate with dimensions of 75 × 5 × 0.5 mm^3 by the diffusion annealing technique, detailly described elsewhere [10,12-14]. The long side of the bidomain plate was perpendicular to the non-polar a-axis (x_1 in crystal physics notation) of the $LiNbO_3$ crystal, thus the piezoelectric constant related to the bending deformation was $(d'_{23})_{y+128°}$, Young's modulus was $(E'_{Y33})_{y+128°} = 1/s'_{3333}$, dielectric permittivity was $(\varepsilon'^T_{22})_{y+128°}$ (assuming the notation $a, x \to x_1;\ y \to x_2;\ c, z \to x_3$). After the heat treatment we deposited tantalum electrodes onto the opposite faces of the bidomain lithium niobate crystal by DC magnetron sputtering.

In order to fasten the bidomain crystal, we used two gaskets and two clamps made of polycrystalline alumina and fixed the structure onto a rigid base with two stainless-steel screws and nuts as it shown in Fig. 1. Two strips made of aluminum foil pressed by clamps to the tantalum electrodes were used for transferring the generated voltage to a coaxial cable and then to the measuring system. The length of the fastened cantilever was 71 ± 0.5 mm.

In order to excite vibrations with ultra-low magnitude and frequency (down to 0.1 nm and 1 Hz, respectively) we used a home-made piezoelectric shaker based on two similar PZT tubes (ceramic type APC 850, APC International Ltd., USA), that were placed vertically on a massive steel plate fixed on a pneumatically stabilized optical table (Standa Ltd., Lithuania). The sensor prototype was mounted on a light aluminum platform fastened on top of the PZT tubes. Finally, the sensor was shielded by a grounded copper box to reduce the electromagnetic noise from external sources.

Mechanical vibrations were excited by applying an AC voltage from an external signal generator to the PZT tubes connected in parallel. In the present study we used only pure sine excitations with low magnitudes and frequencies (less than 10 V and 150 Hz, respectively), so that the excitation of the PZT tubes was always linear with respect to the applied AC signal.

In addition, the reference specimen with dimensions of 10 × 10 × 0.5 mm^3 was cut from the same commercial wafer and annealed together with the sample to be used in the cantilever in order to estimate the width of the interdomain region into the formed bidomain ferroelectric structure. After annealing, an angle lap of the reference specimen was prepared and etched in a $HF : HNO_3 = 2 : 1$(vol.) mixture for the visualization of the domain structure according to [15]. The micrograph of the etched angle lap is shown in Fig. 3. We estimate the width of the interdomain region to be ca. 50 μm which is 10 % of the thickness of the plate. Due to the location of the interdomain region in the center of the bidomain crystal we can take both values Δh_1 and Δh_2 to be equal to 25 μm.

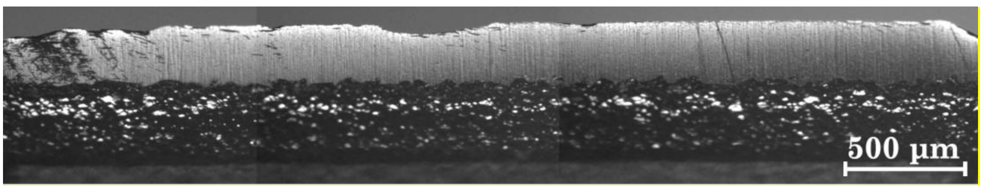

Fig. 3 – A fragment of the panoramic photograph of an etched angle lap prepared in the reference specimen that was annealed in the same run as the bidomain crystal used in the cantilever

We measured the sensor response to the external mechanical vibrations using the lock-in detection of the voltage amplitude by a SR-830 amplifier (Stanford Research Systems Inc., USA). The frequency response data measured by the amplifier was collected to a computer through a 82357B GPIB interface (Keysight Technologies, Inc. USA). The measurement system we used is schematically in Fig. 4. All the lock-in data were obtained with a sine sweep with a step of 0.25 Hz and a bandwidth of the input low-pass filter of 0.23 Hz, with an averaging of 1000 points at each frequency. After collecting all the experimental data was recalculated considering impedances of the bidomain crystal and measuring equipment in order to obtain open-circuit voltage generated by the vibrating cantilever.

More detailed information for measurements and processing of the experimental data can be found in [10]. The parameters for the calculation are given in Table 1.

Because we did not used any seismic mass in our experiments, the term $m_1/\overline{m}$ in equation (18) simply equals 3/2. Young's modulus along the direction defined by a unit vector $\boldsymbol{\zeta} = (\zeta_1; \zeta_2; \zeta_3)$ in $3m$ symmetry class can be calculated as follows:

$$\left(E'_{Y33}\right)_\zeta = \left(1-\zeta_3^2\right)^2 s_{11} + \zeta_3^4 s_{33} + \zeta_3^2\left(1-\zeta_3^2\right)\left(2s_{13}+s_{44}\right) + 2\zeta_2\zeta_3\left(3\zeta_1^2-\zeta_2^2\right)s_{14}. \quad (19)$$

In the crystal wafer of the y + 128° cut the unit vector corresponding to a lateral direction normal to the non-polar axis x_1 equals to $\zeta = (0;\sin(\alpha);\cos(\alpha))$, where $\alpha = 128°$ is the angle of the rotation around the non-polar axis x_1. Thus, Young's modulus in lateral direction normal to the non-polar axis x_1 can be calculated to be $\left(E'_{Y33}\right)_{y+128°}$ = 175 GPa according to equation (19) using the compliance matrix data from [16].

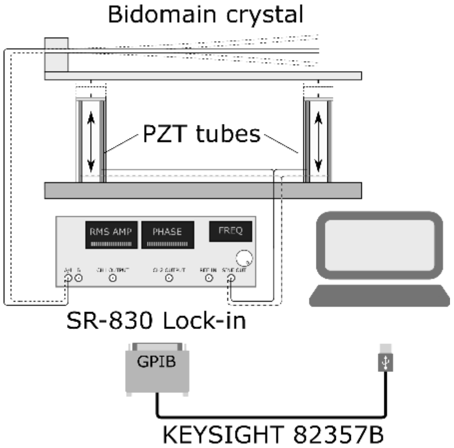

Fig. 4 – Diagram of the lock-in-based technique used for investigations of the sensor in the study (reproduced from [10] under Creative Commons Attribution License CC BY 4.0)

The dielectric permittivity $\left(\varepsilon'^T_{22}\right)_{y+128°}$ for the rotation around the non-polar axis x_1 to the angle $\alpha = 128°$ can be easily calculated as:

$$\left(\varepsilon'^T_{22}\right)_{y+128°} = \varepsilon^T_{11}\cos(\alpha)^2 + \varepsilon^T_{33}\sin(\alpha)^2 = 49.92.$$

The Q-factor can be found from the experimental data by dividing the resonance frequency by the full width at half maximum (FWHM) of the resonance peak in the graph $U^2(f)$, that is shown in Fig. 5. According to these measurements Q = 313.

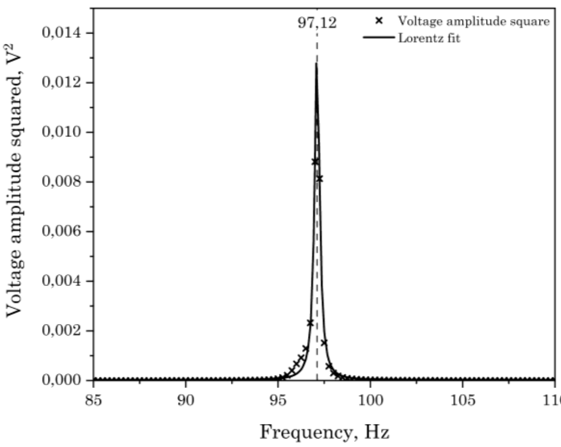

Fig. 5 – Frequency response of the voltage amplitude squared near the resonance frequency (FWHM from the Lorentz fit is 0.31 Hz)

As the resonance frequency is measur ed to be 97.12 Hz, it is possible to estimate Young's modulus of the cantilever by using equation (10). The calculated value is $\left(E'_{Y33}\right)_{meas}$ = 168 GPa, which is quite close to the above mentioned value of Young's modulus derived from the compliance matrix $\left(E'_{Y33}\right)_{y+128°}$ = 175 GPa according to [16] and to the same parameter $\left(E'_{Y33}\right)_{y+128°}$ = 170 GPa obtained by Pendergrass [17]. The difference between these three values can be explained by a possible change in the crystal composition during the diffusion annealing, as well as by the strong dependence of Young's modulus estimated using equation (10) on the length ($\left(E'_{Y33}\right)_{meas} \sim L^4$, therefore a small error in measuring the length leads to a significant change of the computed value of Young's modulus).

Table 1 – Geometric and material parameters of the bidomain $LiNbO_3$ single-crystal used for the calculations

Parameter	Value	Reference
Length, L, mm	71 ± 0.5	
Thickness, H, mm	0.5	
Width, W, mm	5	
Vibrational displacement amplitude, d_0, nm	0.1, 1, 10, 100	
Thickness of the lower polydomain region, Δh_1, μm	25	
Thickness of the upper polydomain region, Δh_1, μm	25	
Q-factor	313	
Resonance frequency, f_0, Hz	97.12	
Elements of compliance matrix, s^E_{ij}, TPa^{-1}	s^E_{11} = 5.78 s^E_{33} = 5.02 s^E_{44} = 17.0 s^E_{13} = −1.47 s^E_{14} = −1.02	[16]
Piezoelectric coefficient, $\left(d'_{23}\right)_{y+128°}$, pC/N	26	[9]
Dielectric permittivity along optical axis, ε^T_{33}	84.45	[18]
Dielectric permittivity perpendicularly to optical axis, ε^T_{11}	28.85	[18]

Fig. 6 displays the frequency response of the cantilever based on the bidomain $LiNbO_3$ crystal to the vibration of the base in the entire investigated range. The experimental data are in a good agreement with the frequency response modelling (obtained from equation (18)). The difference between the graphs is lower than 20 % in almost all points and can be minimized to less than 1 % by changing material parameters, e.g. Young's modulus, piezoelectric coefficient and dielectric permittivity, which can differ from the literature data due to the use of thermally treated out-diffused crystals in this study. The most important observation is that the shape of the modelled frequency response is the same as the shape of the experimental graphs both in the low-frequency and after-resonance region.

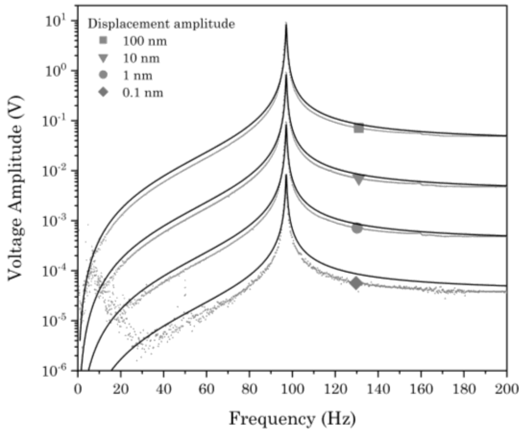

Fig. 6 – Frequency responses of the cantilever made of a bidomain $LiNbO_3$ single-crystal (gray dots) and results of modelling using equation (18) (black solid lines) being subject to sine vibrational excitations with different displacement amplitudes

4. CONCLUSIONS

In the study we suggested a model suitable for vibration sensors of energy harvesters based on ferroelectric bidomain single-crystal plates fastened as a cantilever. We considered a harmonic movement of the base with the cantilever in the direction perpendicular to the plate excited by some external vibrational source. We calculated the vertical displacement of the cantilever's tip depending on the frequency and magnitude of the vibration. The voltage between the electrodes of the cantilever was determined as the integral of the work done by the electrostatic force transferring a single charge in a solid which contains two ferroelectric domains with oppositely directed spontaneous polarization vectors, as well as a polydomain region between the domains. The obtained analytical equation was used to model the frequency response of the device. The result was compared with the experimental data collected using a lock-in and a home-made shaker tool. The material parameters such as Young's modulus, piezoelectric coefficients and dielectric permittivity were obtained from the literature considering the y + 128°-cut of the lithium niobate bidomain plate. We showed a high coherence of the modelled and experimental data, particularly, the shape of the frequency response graph both at low (~10 Hz) and high (at least twice the resonance) excitation frequencies. Meanwhile, this coherence holds in a wide range of excitation amplitudes, at least from 0.1 nm to 100 nm. The numerical disagreements between the computed and measured results can be explained by the difference between the parameters of $LiNbO_3$ obtained for calculation from literature and properties of the cantilever we used. Indeed, the depletion of lithium during the diffusion annealing which we utilized to form bidomain ferroelectric structure may be accompanied by a significant change of the piezoelectric coefficient $(d'_{23})_{y+128°}$, dielectric permittivity $(\varepsilon'^T_{22})_{y+128°}$ and Young's modulus $(E'_{Y33})_{y+128°}$ relatively to the literature data [19].

The modelling results predicts a very high sensitivity of the vibration sensors based on lithium niobate bidomain crystals. Moreover, the high Curie temperature, absence of hysteresis and creep between deformation and generated voltage, as well as a high Q-factor make the bidomain crystals promising for the usage in high temperature sensors and energy harvesters [20].

ACKNOWLEDGEMENTS

The study was supported by the Ministry of Education and Science of the Russian Federation (Federal Targeted Programme for Research and Development in Priority Areas of Development of the Russian Scientific and Technological Complex for 2014-2020) (Project ID RFMEFI57816X0187).

REFERENCES

1. C. Wei, X. Jing, *Renew. Sustain. Energ. Rev.* **74**, 1 (2017).
2. R. Patel, S. McWilliam, A.A. Popov, *Smart Mater. Struct.* **20**, 085004 (2011).
3. A. Pasharavesh, M.T. Ahmadian, H. Zohoor, *Int. J. Mech. Mater. Des.* **13**, 499 (2017).
4. S. Sun, P.W. Tse, *Appl. Phys. Lett.* **110**, 243902 (2017).
5. X. Li, D. Upadrashta, K. Yu, Y. Yang, *Energ. Convers. Manag.* **176**, 69 (2018).
6. A. Erturk, D.J. Inman, *Piezoelectric Energy Harvesting* (John Wiley & Sons, Ltd: Chichester, UK: 2011).
7. S. Bukhari, M. Islam, A. Haziot, J. Beamish, *J. Phys. Conf. Ser.* **568**, 032004 (2014).
8. I.V. Kubasov, A.M. Kislyuk, A.S. Bykov, M.D. Malinkovich, R.N. Zhukov, D.A. Kiselev, S.V. Ksenich, A.A. Temirov, N.G. Timushkin, Y.N. Parkhomenko, *Crystallogr. Rep.* **61**, 258 (2016).
9. I.V. Kubasov, A.V. Popov, A.S. Bykov, A.A. Temirov, A.M. Kislyuk, R.N. Zhukov, D.A. Kiselev, M.V. Chichkov, M.D. Malinkovich, Y.N. Parkhomenko, *Russ. Microelectron.* **46**, 557 (2017).
10. I. Kubasov, A. Kislyuk, A. Turutin, A. Bykov, D. Kiselev, A. Temirov, R. Zhukov, N. Sobolev, M. Malinkovich, Y. Parkhomenko, *Sensors* **19**, 614 (2019).
11. A.V. Turutin, J.V. Vidal, I.V. Kubasov, A.M. Kislyuk, M.D. Malinkovich, N. Parkhomenko, S.P. Kobeleva, A.L. Kholkin, N.A. Sobolev, *J. Phys. D. Appl. Phys.* **51**, 214001 (2018).
12. N. Ohnishi, *Jpn. J. Appl. Phys.* **16**, 1069 (1977).
13. K. Nakamura, H. Ando, H. Shimizu, *Appl. Phys. Lett.* **50**, 1413 (1987).
14. V.D. Kugel, G. Rosenman, *Appl. Phys. Lett.* **62**, 2902 (1993).
15. K. Nassau, H.J. Levinstein, G.M. Loiacono, *Appl. Phys. Lett.* **6**, 228 (1965).
16. A.W. Warner, M. Onoe, G.A. Coquin, *J. Acoust. Soc. Am.* **42**, 1223 (1967).
17. L.L. Pendergrass, *J. Appl. Phys.* **62**, 231 (1987).
18. G. Kovacs, M. Anhorn, H.E. Engan, G. Visintini, C.C.W. Ruppel, *IEEE Symp. Ultrason.*, 435 (IEEE: 1990).
19. J. Kushibiki, I. Takanaga, S. Komatsuzaki, T. Ujiie, *J. Appl. Phys.* **91**, 6341 (2002).
20. F. Chen, L. Kong, W. Song, C. Jiang, S. Tian, F. Yu, L. Qin, C. Wang, X. Zhao, *J. Mater.* (2018).

Моделювання сенсора вібрацій на основі біморфної структури

М.Д. Малинкович[1], І.В. Кубасов[1], А.М. Кислюк[1], А.В. Турутін[1], А.С. Биков[1], Д.А. Кисельов[1], А.А. Теміров[1], Р.Н. Жуков[1], Н.А. Соболєв[1,2], B.M.S. Teixeira[2], Ю.Н. Пархоменко[1]

[1] *Кафедра матеріалознавства напівпровідників і діелектриків, Національний дослідницький університет «МІСіС», 119049 Москва, Росія*

[2] *Department of Physics and I3N, Університет Авейру, 3810-193 Авейру, Португалія*

У дослідженні розроблена математична модель, що описує амплітудно-частотний відгук сенсора або пристрою збору скидної енергії, виготовленого з сегнетоелектричної бідоменної монокристалічної пластини, по відношенню до величини вібраційного збудження. Математична модель дозволяє прогнозувати залежність напруги на електродах від частоти і амплітуди вібраційного збудження, а також резонансної частоти сенсора, що представляє собою прямокутну пластину, в загальному випадку з сейсмічної масою на вільному кінці, який встановлюється на вібраційному столику, параметри коливань якого задаються. Складено відповідне диференційне рівняння, що описує шукані залежності, і отримано його аналітичне рішення. Для перевірки запропонованої моделі був створений монокристалічний біморф за допомогою відпалу підкладки з ніобату літію ($LiNbO_3$) на повітрі для оберненої дифузії літію і формування бідоменної структури, що представляє собою два зустрічно поляризованих домени в одній пластині (так звана структура «голова-до-голови»). Такий кристал аналогічний біморфу, проте на відміну від нього не містить будь-яких міжфазних меж, за винятком міждоменної. Таким чином, виготовлений біморф являє собою не поширену збірну конструкцію, що складається найчастіше з металевої підкладки, до якої прикріплені п'єзоелектричні пластини, як правило, з п'єзокераміки, а однорідне безперервне середовище. Перевага такого біморфу полягає у тому, що, будучи виготовленим з сегнетоелектричного монокристала ніобату (або танталата) літію, сенсор або пристрій збору скидної енергії має великий коефіцієнт перетворення деформації згинання в електричну деформацію, а отже, високу чутливість, а також широкий температурний діапазон застосування та практично повну відсутність гістерезису і старіння. Проведено порівняння результатів моделювання з експериментальними даними, з якого випливає, що запропонована модель добре відповідає результатам експерименту. Показано, що сенсори коливань на бідоменних монокристалічних пластинах мають виключно високу чутливість. Запропонована модель дозволяє оцінювати і прогнозувати параметри сенсорів вібрації, акселерометрів і пристроїв збору скидної енергії на основі бідоменних сегнетоелектричних кристалів.

Ключові слова: Біморф, Бідоменний кристал, Сенсор вібрації, Збір скидної енергії, Моделювання.